Graphene Oxide: A Novel 2-Dimensional Material in Membrane Separation for Water Purification

Article *in* Advanced Materials Interfaces · March 2017

DOI: 10.1002/admi.201600918

CITATIONS
92

READS
859

5 authors, including:

Mahdi Fathizadeh
University of South Carolina
40 PUBLICATIONS **1,574** CITATIONS
SEE PROFILE

Weiwei Xu
Gas Technology Institute
22 PUBLICATIONS **784** CITATIONS
SEE PROFILE

Fanglei Zhou
Membrane Technology and Research, Inc.
23 PUBLICATIONS **811** CITATIONS
SEE PROFILE

Yeomin Yoon
University of South Carolina
228 PUBLICATIONS **13,450** CITATIONS
SEE PROFILE

ADVANCED MATERIALS INTERFACES
www.advmatinterfaces.de

Graphene Oxide: A Novel 2-Dimensional Material in Membrane Separation for Water Purification

*Mahdi Fathizadeh, Weiwei L. Xu, Fanglei Zhou, Yeomin Yoon, and Miao Yu**

As a newly emerging 2-dimensional (2-D) material with sub-nanometer thickness, graphene oxide (GO) has been widely studied either as a pure/skeleton membrane material or as an additive in and a functional coating on matrix membranes for water purification because of its unique physico-chemico-mechanical properties. Manipulating or incorporating this novel 2-D material effectively into a membrane structure has been shown to significantly improve membrane performance, including increased water permeability, alleviated fouling, improved antibacterial properties, etc., which will eventually lead to lower energy consumption, longer lifetime, and lower maintenance cost. As the pure/skeleton membrane material, GO flakes typically are deposited as a lamellar structure by solution-based coating processes on appropriate porous supports, and nano-channels between GO sheets and sometimes structural defects within GO could be utilized as transport passage. As an effective additive and surface functional coating, GO also shows great potential to improve water permeation, surface hydrophilicity, and chemical resistance. In this paper, the latest studies on the use of GO in membrane application for water purification are reviewed, and potential challenges are discussed. Moreover, possible future research directions to further develop GO or GO-incorporated membranes for water purification are suggested in different membrane separation processes.

1. Introduction

Graphene oxide (GO) is an oxidized form of graphene that is made of carbon atoms bonded in hexagonal honeycomb lattice. Due to the strong oxidation conditions during its synthesis, for example, by Hummers[1] or Staudenmaier[2] method, a large amount of oxygen-containing groups, including epoxide, hydroxyl, and carboxylic acid groups, exist in GO, as shown in **Figure 1**. These functional groups lead to good hydrophilicity and allow excellent dispersion of GO flakes in water. This, as a significant advantage, greatly facilitates GO deposition from solution using water as a low cost and environment-friendly solvent.[3] Recently, GO has attracted great attention as a novel 2-D membrane material in water purification application because of its excellent mechanical property, atomically thin thickness, excellent dispersion in water, and ease to form compact membrane structure or to be added into polymer matrix.[3,4]

Concept demonstration/preliminary studies on using graphene-based membranes for water purification were focused on simulations for single layer graphene/GO/reduced GO (rGO) with structural defects. Cohen-Tanugi et al.,[5] using molecular dynamics (MD) simulation, found that hydrogenated and hydroxylated defects with appropriate sizes on graphene could have 2–3 orders of magnitude higher water permeability than commercial reverse osmosis (RO) membranes but similarly high salt rejection, suggesting great potential of single-layered graphene membranes for desalination. Lin et al.[6] showed by MD simulations that thermally reducing GO with different initial epoxy to hydroxyl ratios and different oxygen concentrations may generate selective defects on rGO for high water permeability and high salt rejection desalination. **Figure 2**a shows representative structures of rGO after reduction at 2,500 K, when GO flakes with different starting oxygen concentrations and epoxy concentrations or epoxy/hydroxyl ratios are used. With the increase of oxygen concentration and epoxy concentration, rGO becomes more defective and has bigger nanopores because of more carbon removal from the GO matrix. This suggests pores on rGO may be controlled by controlling starting GO composition and reduction conditions. Further, they studied desalination performance of defects on rGO after reduction at different temperatures and using GO with different oxygen concentrations and epoxy concentrations (Figure 2b). Too low oxygen concentration (17%) leads to complete water blocking irrespective of reduction temperature and initial epoxy concentration or epoxy/hydroxyl ratio. At higher initial oxygen concentration (25% and 33%), high water flux and 99% salt rejection can be obtained depending on reduction temperature epoxy/hydroxyl ratio. These promising simulation results, therefore, suggest appropriately reducing GO with desired starting composition

M. Fathizadeh, W. L. Xu, F. Zhou, M. Yu
Department of Chemical Engineering and Catalysis for Renewable Fuels Center
University of South Carolina
Columbia, SC 29208, USA
E-mail: yumiao@cec.sc.edu
Y. Yoon
Department of Civil and Environmental Engineering
University of South Carolina
Columbia, SC 29208, USA

DOI: 10.1002/admi.201600918

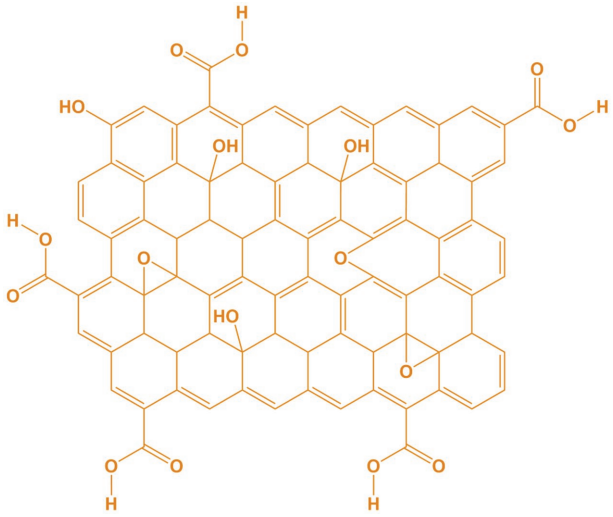

Figure 1. Chemical structure of graphene oxide (GO) composed of a graphene sheet derivatized by phenyl epoxide and hydroxyl groups on the basal plane and carboxylic acid groups on the edge.

may lead to high performance desalination membranes. In another study, permeation of water and ions through functionalized and un-functionalized pores of single layer graphene sheet was investigated using MD simulations.[7] They found that pristine pores with diameter approximately 0.75 nm can effectively exclude ions, whereas ion rejection decreased with the increase of ion concertation and pore diameter. Comparison among carboxyl anion, amine cation, and hydroxyl groups indicated that carboxyl group had better ion rejection, particularly for Cl^-.

To experimentally demonstrate the feasibility of utilizing structural defects for selective water permeation, several clever experiments have been designed. Surwade et al.[8] covered a 5-μm pore with a single layer of graphene with a grain size of 50 μm, and then applied very short time (<10 s) oxygen plasm etching to create nanopores; their results indicated that under certain etching conditions, generated defects had an extremely high water permeability, about 1,000 times higher than commercial RO membranes, and approximately 100% salt rejection. O'Hern et al.[9] transferred single layer graphene grown by chemical vapor deposition to a porous polycarbonate substrate and then used ion bombardment and oxidative etching to tune defects sizes on graphene in the sub-nanometer range and thus allow slat transport while excluding organic dye molecules. These experimental studies seem to support the simulation results and show the potential of the structural defects within graphene. However, it is very challenging to make macroscopic, single-layered graphene or GO membranes that have desired structural defects that are the only transport pathway and only allow water permeation.

Another parallel pathway of using GO in membrane fabrication is to form lamellar structure and utilize nano-channels between GO flakes for selective water permeation. As the very first study, in 1961 Boehm et al.[10] synthesized graphite oxide and prepared membranes by evaporation of its suspension on a porous glass plate, and investigated water vapor permeation and ion diffusion. Bober et al.[11] studied desalination performance of the deposited graphite oxide membranes, and found a membrane with thickness of approximately 300 nm had high rejection for NaCl (≈90%) but low water permeance

Dr. Mahdi Fathizadeh currently is a postdoc fellow at the University of South Carolina. He obtained BS, MS and PhD degrees from Amirkabir University of technology, Iran, all in Chemical Engineering. He also majored in polymer science as his second major during his undergraduate study. Prior to joining USC, he worked at Shimi Sanat Gostar Amirkabir, Inc., a start-up company he co-founded to commercialize RO membranes. He also worked as an assistant professor at Ilam university, Iran from 2012-2014 with the focus on RO, NF and UF membranes for water treatment and purification.

Weiwei L. Xu is currently a PhD candidate in the Department of Chemical Engineering at the University of South Carolina. He received his Bachelor's degree in Chemical Engineering from Jilin University (P.R. China), and his Master's degree in Organic Chemistry from the Chemistry Department of the University of South Carolina. In 2014, he joined Dr. Yu's group and focused his research on the fundamental understanding of graphene oxide (GO) based membranes and the development of ultrathin GO membranes for water purification and gas separation.

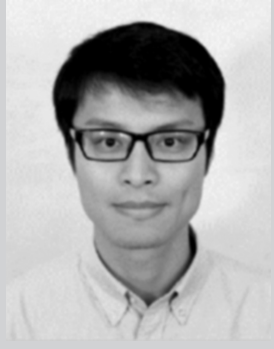

Fanglei Zhou received his Bachelor's and Master's degree in Chemical Engineering from Wuhan Institute of Technology in 2010 and 2013, respectively. He worked in Membrane R&D Department in Alfa Laval, Nakskov, Denmark from 2012 to 2013 and Membrane Science, Engineering and Technology (MAST) Center at the University of Arkansas, US from 2014 to 2015. Then he joined Dr. Yu's group as a PhD student at the University of South Carolina in 2015. His main research is focused on GO-based membrane fabrication and its application on gas and liquid separation.

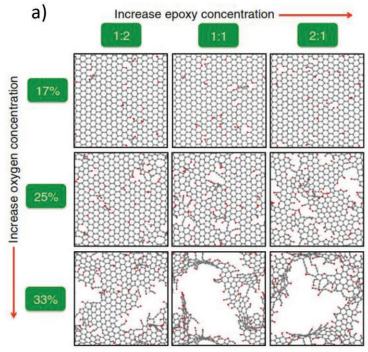

b)

Initial oxygen concentration		Water flux (L cm^{-2} day^{-1} MPa^{-1}) 1:2*	1:1*	2:1*	Salt rejection (%) 1:2	1:1	2:1
T= 1500 K	17%	0.0	0.0	0.0	100	100	100
	25%	0.0	0.0	0.0	100	100	100
	33%	0.0	2.6	2.0	100	99	100
T= 2000 K	17%	0.0	0.0	0.0	100	100	100
	25%	0.0	0.0	0.1	100	100	100
	33%	2.1	15.3	(L)	100	99	(L)
T= 2500 K	17%	0.0	0.0	0.0	100	100	100
	25%	0.0	0.0	15.4	100	100	93
	33%	27.4	(L)	(L)	94	(L)	(L)
T= 3000 K	17%	0.0	0.0	0.0	100	100	100
	25%	0.1	3.0	(L)	100	100	(L)
	33%	(L)	(L)	(L)	(L)	(L)	(L)

*Initial epoxy/hydroxyl ratio. The letter '(L)' indicates that nanopores in rGO membranes are too large and both the water molecules and salt ions can freely pass through the rGO membrane

Figure 2. a) Representative defective structures of rGO after reduction at 2,500 K. The epoxy/hydroxyl ratio and initial oxygen concentration of GO sheets are shown along the horizontal and vertical directions, respectively. All structures are represented as ball and stick with carbon, oxygen and hydrogen atoms in grey, red and white color, respectively. b) separation performance of rGO membranes in water desalination.[6] Copyright 2015, Nature Publishing Group.

(0.04 L (m^2 h bar)$^{-1}$) at 600 psi. After 50 years, Nair et al.[12] fabricated approximately micrometer-thick, free-standing GO membranes and found that water vapor permeated through the membrane with negligible transport resistance, but even helium can't permeate through the dry membrane; they also found small organic molecules, such as methanol, acetone, and hexane etc., had several orders of magnitude lower permeability than water. In a following study in 2014,[13] they observed, by liquid phase diffusion experiments, thick GO membranes exhibited a sharp cutoff size of nano-channels at ≈0.9 nm; species with hydrated radius lager than ≈0.45 nm were sieved out, whereas small species, such as K^+, Mg^{2+} and AsO_4^{3-} ions, permeated with approximately the same rate and showed weak dependence on ion charge (**Figure 3**). These promising preliminary results demonstrated

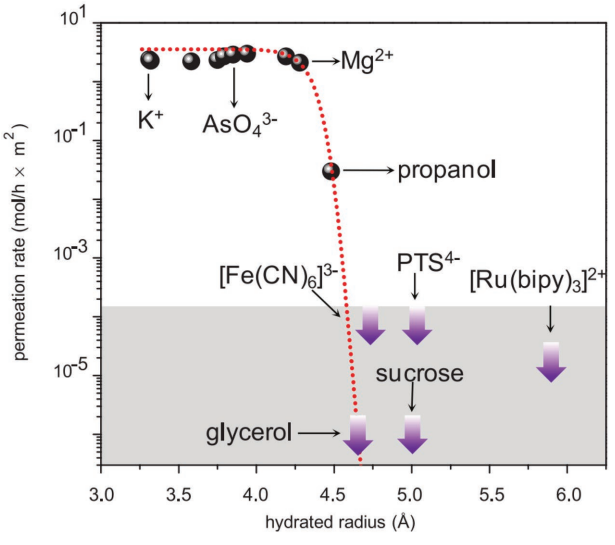

Figure 3. Permeation rate of ions and neutral molecules with different hydrated radius through GO membranes. Permeation rates are normalized per 1 M feed solution and measured by using 5-µm-thick membranes. Reproduced with permission.[13] Copyright 2014, IOP.

that nano-channels between GO flakes have great potential for highly selective water permeation, and stimulated extensive study of using GO membranes with lamellar structure for water purification. The enhanced water permeability through membranes composed of multiple GO flakes with pores within the flakes and having lamellar structure was studied using atomistic simulations and theoretical analysis to understand the observed water permeation behavior.[14] The physical picture of ultrafast flow between pristine graphene sheets breaks down due to a side-pinning effect by water confined between oxidized regions in GO membranes. Generally, expanded interlayer gallery, wide channels formed at wrinkles, holes, and interedge spaces could prominently improve water flow in GO sheets.[14]

Encouraged by the exciting preliminary experimental demonstrations and simulations, researchers from all over the world are exploring various ways of utilizing 2-D GO to improve membrane performance in water purification. There are three typical ways of fabricating GO-incorporated membranes: i) lamellar-structured membranes with GO as the skeleton material; ii) mixed matrix membranes (MMM) with GO as the additive; and iii) GO surface functional coatings. **Figure 4** shows representative membrane structures formed via these three ways. In structure I, nano-channels between GO flakes in parallel dominate the molecular permeation, and current research is focused on modifying GO surface properties, controllably depositing GO flakes to form more ordered lamellar structure, and tuning the nano-channel size (physically and chemically).[14–16] In structure II, GO serves as a functional additive to modify the properties of the matrix membrane (typically hydrophobic), such as hydrophilicity and surface roughness, to improve surface hydrophilicity and antifouling performance, and/or to introduce extra transport pathways.[14,16] In structure III, GO acts as a functional coating that changes the contacting material with the feed liquid, and thus may work as a protective layer, antibacterial and antifouling coating.[14,16,17] In this review, we discuss research progress on these three structures involving GO, point out potential problems, and finally suggest future research directions.

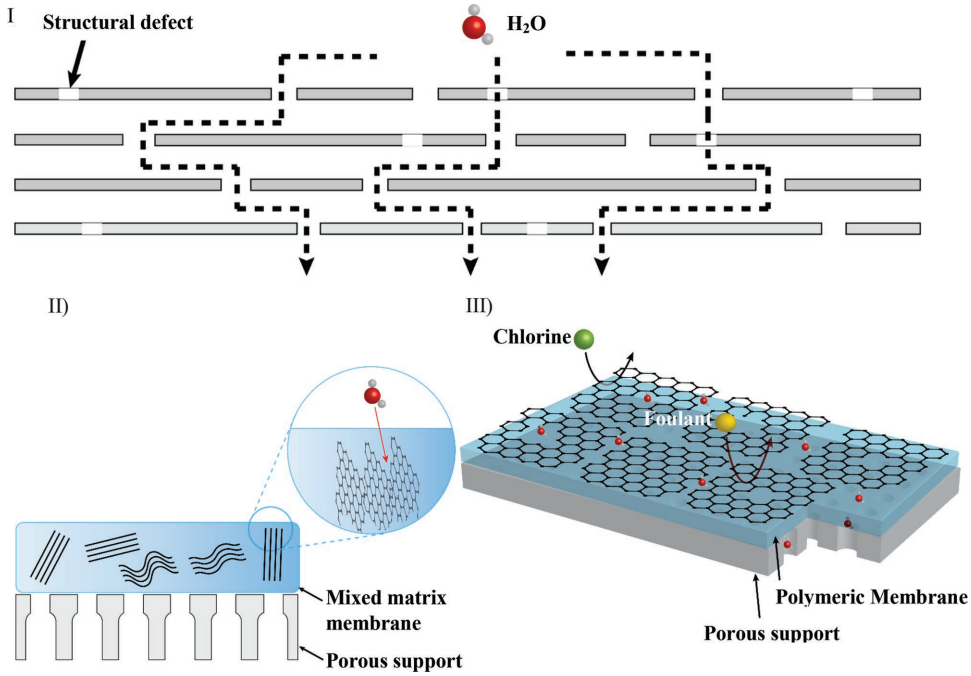

Figure 4. Three representative membrane structures with incorporated GO flakes: I) GO-based membranes with lamellar structure; dashed lines indicate transport pathways of water molecules (a water molecule was shown on top of the membrane surface), and white channels within GO flakes (grey slab) are structural defects; II) mixed matrix membranes (MMM) with GO as the additive; light blue indicates the bulk matrix material, and groups of black lines indicate agglomerates of GO flakes; and III) GO functional coating on polymeric membrane.

2. GO-Based Membranes with Lamellar Structure

An ideal graphene-based membrane would be composed of just one layer of graphene or GO with desired structural defect size and high porosity to provide high water selectivity and high permeability. However, as we discussed above, only very limited studies have been conducted along this pathway. This is because i) there lacks simple and reliable methods for fabricating single-layered graphene or GO membranes and ii) it is very difficult to control structural defect sizes and porosity. In contrast, pure/free GO membranes with lamellar structure can be prepared by facile solution-based deposition processes, and initial permeation studies using thick GO membranes with lamellar structure have shown potential of nano-channels for selective water permeation.[12,13]

Pure/free GO membranes with lamellar structure, however, may have potential stability problem, resulting from the swelling in water and other solvents and weak mechanical strength. Two major strategies are adopted to solve the potential stability issue of hydrophilic GO membranes in an aqueous environment. The first strategy is the layer-by-layer (LBL) assembly via electrostatic interactions, while the second one is to create covalent bonding between GO flakes using cross-linking agents. Although, LBL assembly via electrostatic interaction can partially improve the stability of GO membranes and membrane performance, they are still susceptible for swelling in water and organic solution because of the charge screening effect. In contrast, chemically bonded GO membranes can be a good alternative for enhancing membrane performance and stability. Organic agents, such as diamine monomers, have been successfully employed as cross-linking agents. **Figure 5**a shows LBL assembly preparation steps of GO sheets with polyethyleneimine (PEI) membrane; the electrostatic interactions between positively-charged PEI and negatively-charged GO improved stability of GO layers.[18] Figure 5b illustrates a schematic of utilizing covalent reaction between GO sheets and 1, 3, 5-benzenetricarbonyl trichloride (TMC) monomers to form stable GO-based membranes.[19]

2.1. Pure GO Membranes with Lamellar Structure

Following the work of thick pure/free GO membranes with lamellar structure, extensive studies were conducted to further investigate the potential of free GO membranes with lamellar structure for water purification. Similar selective ion diffusion was reported by Sun et al.;[20] they found a micrometer-thick (<10 μm) free standing GO membrane separated Na^+ from Cu^{2+} due to the strong coordination interaction between heavy-metal ions and oxygen-containing functional groups of GO. Furthermore, organic contaminates, such as rhodamine B, were completely blocked by the membrane because of their strong interactions with oxygen containing functional groups on the GO sheets. Huang et al.[21] studied effects of feed pressure during GO filtration deposition, pH, and salt concentration on water filtration performance of GO membranes with thickness around 500 nm. They reported that low pH and high pressure around 1.3 MPa led to the lowest water permeability but the highest Evans blue (EB) dye rejection, resulting from the narrowed interlayer spacing/nano-channels under these

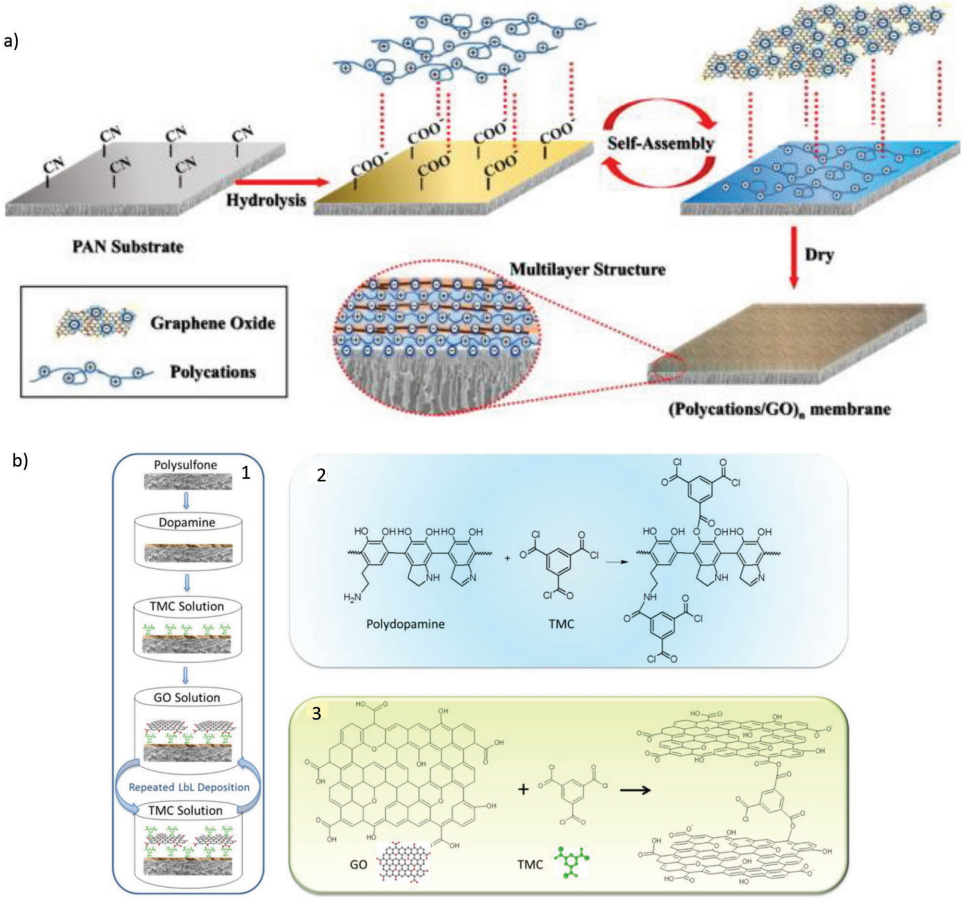

Figure 5. Strategies of improving GO-based membrane stability: a) LBL membrane preparation by electrostatic interaction between polycation and GO on PAN support. Reproduced with permission.[18] Copyright 2016, Elsevier. b) covalent interaction: (1) a step-by-step procedure to synthesize the GO membrane, (2) reaction between polydopamine and TMC, and (3) reaction between GO and TMC. Reproduced with permission.[19] Copyright 2013, ACS.

conditions. At pH 3, the permeability of this freestanding GO membrane was 12.19 L $(m^2\ h\ bar)^{-1}$, approximately 15 times higher than commercial RO membrane, with 100% rejection of EB dye. Low pH and high salt concentration were found to lower the repulsion forces between the negatively charged GO sheets and thus dramatically decrease nano-channel size between GO flakes, which led to the decrease of the flux and increase of the dye rejection. High applied pressure also decreased interlayer spacing between GO flakes, and as a result water flux decreased and dye rejection increased. The "squeezed" nano-channels under high pressure, however, can be recovered by releasing the applied pressure due to the unique elastic properties.[21]

The above discussed work clearly showed potential of pure GO membranes with lamellar structure for selective water permeation. However, water permeability was still low due to the thick membrane thickness and thus long transport pathway. A natural step to proceed is to develop thinner GO membranes and investigate their potential for water purification. Effect of GO layer thickness on desalination performance was studied by Deng et al.[22] They found that GO membranes thinner than 30 nm had a high water flux but low salt rejection (< 5%). Increasing thickness of GO membrane from 30 nm to 300 nm decreased water flux from 1650 to 250 L $(m^2\ h\ bar)^{-1}$ and increased NaCl rejection from less than 5% to approximately 15%. Their results suggested that increasing GO membrane thickness can increase the salt rejection, but it is still way lower than polymeric RO membranes. They speculated that thicker GO membranes may have more organized lamellar structure and smaller interlayer spacing. Higher rejection for hydrated Na^+ by pure GO membranes with lamellar structure is expected if GO interlayer spacing can be reduced to be less than 0.7 nm, for example, by partially reducing GO. Han et al.[23] reported ultrathin (22–53 nm) rGO membranes for nanofiltration (NF). Their membranes were fabricated by vacuum filtration of base-refluxing reduced GO (brGO) dispersion on porous substrates (anodic alumina oxide (AAO) disks or Polyvinylidenefluoride (PVDF) membranes); membrane thickness was controlled by GO loading per membrane area. Accompanied with pure water permeability as high as 21.8 L $(m^2\ h\ bar)^{-1}$, the resulting membranes showed >99% rejection for large organic dyes, such as methyl blue (MB) and direct red 81 (DR). Moreover, the ultrathin rGO membranes exhibited moderate rejection (20–60%) for salts with different cation to anion charge ratios. They suggested that rejection of organic dyes was attributed to the combined effect of size sieving and electrostatic interaction, whereas Donnan exclusion

dominated the salt rejection. In another study, ultraviolet (UV) reduction was used to overcome the swelling of hydrated GO membranes.[22] Under UV irradiation, GO flakes were gradually reduced to rGO, resulting in a narrowed interlayer spacing. Salt rejection rates increased slowly with UV irradiation time. NaCl rejection (28%) by rGO membrane after UV irradiation for 4 days was 1.5 times higher than that of GO membrane. Their results suggested that partial reduction can narrow interlay spacing, and thus increase salt rejection.

Moreover, rGO-based membranes were also studied for forward osmosis (FO) application. As a low energy consumption process (no hydraulic pressure needed), FO has attracted great attention over the past decade as an alternative desalination method for a conventional pressure-driven RO process. Membrane support selection is very important for FO membrane performance, because the internal concentration polarization (ICP) could significantly reduce membrane permeability and aggravate fouling. Liu et al.[24] reported the fabrication of ultrathin (100 nm), freestanding rGO FO membranes which greatly alleviated the ICP issue brought by FO membrane support. In this novel membrane fabrication strategy, hydrogen iodide (HI) steam worked as a reducing agent for the GO membrane, which also triggered the peeling of rGO membrane from cellulose acetate substrate as immersing into water. The resulting freestanding rGO membrane showed high mechanical stability, which makes it suitable for FO application. The water permeability of the freestanding, 100 nm rGO FO membrane reached 57.0 L m^{-2} h^{-1}, while using water as feed and NaCl (2.0 M) as the draw solution. Water permeability of the membrane also exhibited linear increase with the increase of the draw solution concentration (0.5–2.0 M), suggesting the ICP was almost eliminated. After 12 h FO operation, the reverse NaCl flux was measured to be 0.02 mol $(m^2\ h)^{-1}$. The freestanding rGO FO membrane also showed high rejection for acid orange 7 and Cu^{2+}.

Considering the nanometer-sized 2-D channels and surface hydrophilicity, ultrathin GO membranes were also studied for their potential for waste water treatment. Song et al.[25] conducted the filtration test of water containing a typical natural organic matter, humic acid (HA), using GO membranes (5–30 nm thick) supported on porous polyethersulfone (PES). They found that hydrophilic GO membrane surface enhanced water permeability and fouling resistance, and nano-channels of GO membranes also increased rejection for HA from 20% for pristine PES support to 80% for GO membrane.

Besides removing salt and organic contaminants in water by size sieving and/or electrostatic repulsion, hydrophilic nanochannels in GO membranes with lamellar structure were also explored for selective extraction of water from organic solvents by pervaporation (PV). The sorption-diffusion mechanism plays a key role on molecular permeation in PV. Many researchers investigated potential of GO membranes with lamellar structure for organics dehydration, and found that nano-sized interlayer spacing between GO flakes can act as selective nanochannels for water permeation in PV.[26–29] **Table 1** summarizes recent results of GO-based membranes for organic dehydration by PV. In the following, we will discuss some representative results in more details.

Generally, PV performance of GO membranes is expected to depend on supporting porous substrate (pore size, material, and surface morphology etc.), interlayer spacing between GO flakes, GO layer thickness, and the functional groups on GO. Proof of concept studies were performed to show potential of GO membranes with lamellar structure for selective water extraction. Huang et al.[27] used a GO membrane (thickness: 600–1,600 nm) for ethanol and dimethyl carbonate (DMC)/water separation by PV. They coated a GO layer on a ceramic hollow fiber substrate by vacuum filtration process. Results showed high separation performance of the GO membranes for DMC/water mixture with separation factor of 740 and total permeability of 1702 g $(m^2\ h)^{-1}$. They attributed this to the preferential water sorption ability and fast water diffusivity through the GO layers. Liu et al.[26] found that permeability of alcohols, such as ethanol, 1-propanol and 2-propanol, was about 80 times lower than that of water; as a result, in PV of water/alcohol mixtures, water was preferentially extracted, and thus alcohols with concentration of ≈97% were generated. In these GO membranes, the interlayer spacing between the GO sheets is subnanometer and hydrophilic, and thus allow preferential water permeation. Moreover, structural defects on GO flakes generated during oxidation process may provide additional transport pathway for molecules, and the effect of these defects decreased with the increase of the GO layer thickness because of mutual stacking.[27]

To understand influence of GO membrane preparation conditions and membrane nanostructure on PV performance and thus further improve both water flux and separation factor, various methods for GO deposition or post-treatment were explored. Liu et al.[26] found permeability in PV of ethanol/water mixture decreased more than 20 times with the increase of the drying temperature. Depending on the drying temperature (40–200 °C), the oxygenated groups at the edges of defects and GO flakes surface can create a GO interlayer spacing from sub-0.6 to 1.0 nm. Besides controlling drying temperature of the deposited wet GO membranes, other methods, including pressurization and vacuuming during GO dispersion filtration and evaporation rate control, were adopted by Tsou et al.[29] for preparing GO membranes on modified polyacrylonitrile (mPAN) support. Results revealed that GO membranes with different microstructures resulted; assembled GO membranes by pressurization had the smallest interlayer spacing and the best PV performance (Table 1). The pressure-assisted self-assembly technique was also used by other groups,[35,32] and results were in good agreement with those obtained by Tsou et al. Specifically, they investigated the effect of pressurization on GO membrane fabrication for dehydration of ethanol.[32] Ethanol/water separation performance showed that pressurization improved GO packing density, thereby improving selectivity and decreasing permeability. However, pressure higher than 5 bar led to fast GO deposition rate, which may cause defects in the GO membranes. Hung et al.[33] applied this optimum pressure to deposit a GO layer with highly ordered lamellar structure on polyacrylonitrile (PAN) support for isopropanol/water separation. They studied the effect of GO coating thickness on PV performance, and found that the separation factor of GO membrane increased initially with the coating thickness and then remained unchanged after an optimum thickness of 300 nm. When GO coating was thinner than the optimum thickness, it could not completely cover the support surface, therefore

Table 1. PV performance of GO-based membranes with lamellar structure for water/organics separation.

Organic components	Preparation method	Membrane composition	Conditions	Support layer	Thickness (nm)	Flux ($g\ m^{-2}\ h^{-1}$)	Separation factor	Reference
Methanol and Dimethyl carbonate	Vacuum filtration	GO	t: 25 to 40 °C Water: 1–2.6%	Ceramic hollow fiber	100	1702	740	[27]
Ethanol, methanol, 1-propanol, 2-propanol	Vacuum filtration	GO	t: ≈25 °C Water: 0 to 100%	PTFE	4,500	–	500–700	[26]
Butanol	Vacuum filtration	GO	t: 30 to 70 °C Water: 5 to 15%	AAO	600	3,100	250	[30]
Isopropyl	Vacuum filtration	GO	t: 50 to 70 °C Water: 10%	PVDF	–	1,400	1,500	[31]
1-butanol	Vacuum filtration, pressurization, and evaporation	GO	t: 30 to 70 °C Water: 10%	PAN	300	4340	2241	[29]
Ethanol	Pressurization	GO	t: ≈25 °C Water: 0 to 100%	Cyclopore polycarbonate	10,000	3,500	1450	[32]
Isopropanol	Pressurization	GO	t: 30 to 70 °C water: 30%	mPAN	400	4,137	1,164	[33]
Ethanol	Vacuum spin coating	GO	t: ≈25 °C Water: 20%	PAN	93	500	350	[34]
Ethanol (Eth), n-propanol (NPA), isopropanol (IPA), ethyl acetate (EA)	Vacuum filtration	GO with EDA	t: 70 °C Water: 10%	Ceramic hollow fiber	250	Eth = 1200 NPA = 1400 IPA = 1800 EA = 1900	Eth = 200 NPA = 1000 IPA = 2000 EA = 2500	[28]
Ethanol	Pressurization	GO with diamines	t: 30 to 80 °C Water: 10%	CA	420	2,297	4,500	[35]
Methanol (MET), Ethanol (ETH), n-propanol (NPA), isopropanol (IPA), isobutanol (IBA), secbutanol (SEB), tert-butanol (TBA)	Vacuum filtration	GO with 1,4-phenyldi-boronic acid	t: ≈25 °C Water: 10%	PVA	400	MEH = 450 ETH = 300 NPA = 350 IPA = 220 IBA = 500 SEB = 450 TBA = 350	MEH = 900 ETH = 4000 NPA = 10000 IPA = 20000 IBA = 70000 SEB = 10^5 TBA = 10^5	[36]

separation factor was very low. When GO coating was thicker than the optimum thickness, permeability decreased because of increased mass transfer resistance; but, separation factor kept almost constant.[33] Moreover, they showed that interlayer spacing of GO coating increased during separation process. Hydrogen bonding (H-bonding) and π–π interactions are dominant forces that hold GO flakes together during pervaporation. Intercalation of water and alcohol molecules between GO flakes leads to the substantially increased interlayer spacing, and thus decreases GO membrane PV performance.

2.2. GO Framework (GOF) Membranes

Despite initial promising performance of pure/free GO membranes with lamellar structure for water purification, membrane stability in aqueous solutions may be one potential concern. Pure/free GO membranes have only intermolecular interactions and thus may not be strong enough to provide long-term stability in aqueous phase. As GO is highly dispersible in water, GO membranes may disintegrate during membrane separation, particularly for long time operation. Also, GO flakes become negatively charged on hydration in water, and electrostatic repulsion can dissipate packed GO flakes.[37] Enhancing interactions between GO flakes or introducing chemical bonds between GO flakes are expected to improve GO membranes stability and thus increase their life time. Mixing GO with cross-linking agents, adding charged polymer between GO sheets, and using functionalized GO, therefore, have been studied for preparing more stable GOF membranes with enhanced interactions or chemical bonding between GO flakes.[18,35,37,38]

Hu et al.[19] prepared GO based FO membranes through LBL assembly of GO with poly(allylamine hydrochloride) (PAH) via electrostatic interaction. GO/PAH bilayer was around 16.5 nm thick, and the resulting 10-bilayer GO membrane had water permeability that was 3–4 times higher than commercial HTI membrane developed by Hydration Technology Innovations, LLC. Although reverse flux of ionic species (3.3 mol $(m^2\ s)^{-1}$) of the membrane was not low enough, the rejection of sucrose by the 10-bilayer GO membrane was around 99%. GO membranes prepared by LBL method, therefore, may be suitable for FO separation while using sucrose as drawing solution.

To avoid swelling of GO membranes, chemical bonding was introduced into GO membranes to "lock" GO flakes in the adjacent layers.[19,39,40] GO membranes can also be stabilized using cross-linking agents, such as multivalent ions,[37] diamine, or dyadic monomers.[32,34] Via a LBL deposition technique, TMC was used to cross-link adjacent GO flakes.[19] The resulting stabilized membrane exhibited high permeability

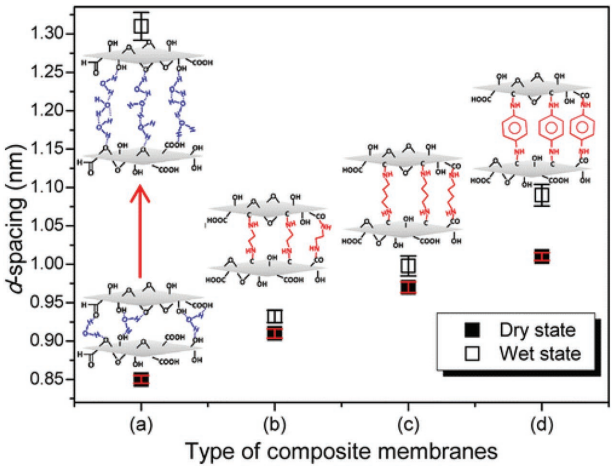

Figure 6. d-spacing/interlayer spacing of GO membranes crosslinked with diamines at the dry and wet states: a) pure GO, b) GO/ethylene diamine, c) GO/butylenediamine, and d) GO/p-phenylenediamine. Reproduced with permission.[35] Copyright 2014, ACS.

ranging from 8 to 27.6 L (m^2 h bar)$^{-1}$. Albeit TMC cross-linked GO membranes did not show high salt rejection (6–46%), they gave a moderate rejection (46–66%) for MB and high rejection (93–95%) for Rhodamine-WT. Besides TMC used by Hu et al.,[19] diamines, as mentioned above, are another type of cross-linkers that could be applied to lock GO flakes and thus improve membrane stability. Xia et al.[39] reported, by using different diamines as cross-linkers, including ethylenediamine (EDA), 1,3-propaneddamine and m-phenylenediamine, the interlayer spacing of GO membrane was fixed at 0.92, 0.96 and 0.98 nm, respectively (**Figure 6**). This greatly improved GO membrane stability. Applying a similar idea, Chung and co-workers[38] used EDA to cross-link GO membrane as well. In addition, hyperbranched polyethylenimine (HPEI) (molecular weight: ≈60,000 g mol^{-1}) was applied to modify the surface of membrane. The amine-modified membrane showed high water permeability of 5.01 L (m^2 h bar)$^{-1}$ and comparable high rejection towards heavy metal ions, such as Mg^{2+}, Pb^{2+}, Ni^{2+}, Cd^{2+}, and Zn^{2+}. To increase the stability of GO layer, Chong et al.[41] firstly introduced a porous poly (methyl methacrylate) (PMMA) sacrificial layer on the hollow fiber support and below GO coating; the space between hollow fiber support and the GO membrane allows stress-free shrinkage. The defect-free GO hollow fiber membranes were subsequently fabricated by removing the sacrificial layer. Upon UV-light irradiation, pure water permeability of GO hollow fiber membranes with 150 nm thickness was greatly enhanced from 0.07 to 2.8 L (m^2 h bar)$^{-1}$; meanwhile, the membranes still maintained low molecular weight cut off ≈250 Da.

Hung et al.[35] studied the stability of freestanding GO membranes in ethanol/water pervaporation using X-ray diffraction (XRD). They showed d-spacing of freestanding GO membranes increased after soaking in different solvents. To prevent the swelling of GO membranes and thus maintain desired interlayer spacing in PV, they used EDA as a cross linker to fix the lamellar structure of GO membranes during PV. They defined these GO membranes with molecular linkers between layers as GOF membranes. The interlayer distance between hydrated GO layers was fixed at 0.89 nm by this cross linker agent. They showed that separation factor increased significantly, particularly for water over larger alcohol, such as n-propanol, isopropanol and butanol. Three other diamine monomers were also employed for cross-linking GO sheets to prepare GOF membranes using a pressure-assisted method on CA substrate.[35] Results of wet and dry conditions of pristine GO and GOF membranes clarified that the interlayer spacing of GOF membranes were more stable than pristine GO membranes. For pristine GO membranes, the solution that entered GO layers destroyed hydrogen bonding and π–π interactions and stretched interlayer spacing or d-spacing. In contrast, the formed C-N bonds between GO carboxylic and linker amine groups can resist interlayer stretching; as a result, separation factor increased significantly from 70 to 4500 for ethanol/water mixture with the maximum water concentration on the permeate side of 99.8%.[35] Also, Li et al.[36] used phenyldiboronic acid as cross-linker to fabricate GOF PV membrane. They found a high stability and excellent PV performance for isobutanol/water mixture with flux around 500 g (m^2 h)$^{-1}$ and separation factor higher than 70,000.

3. GO Composite Membranes and MMM with GO Additive

Although GO-based membranes with lamellar structure showed remarkable performance in various water separation processes as discussed above, they may be limited in NF, RO, and PV due to the sub-nanometer interlayer spacing. To extend the applications of GO-based membranes, for example, to ultrafiltration (UF) and microfiltration (MF), and further improve GO-based membrane performance, various inorganic materials, such as carbon nanotubes (CNTs), TiO_2, Ag[42–44] and other nanoparticles[9,40,43] have been hybridized with GO to improve their water purification performance. In addition, GO has been investigated as a novel additive to various polymers to form MMM with improved water purification performance.[44–48]

3.1. GO/Nanoparticle Composite Membranes

Nanoparticles, such as CNTs, TiO_2, zeolite, etc., have been added to GO membranes to improve their stability or fix interlayer spacing of GO flakes for various water purification processes.[49,50] Han et al.[23] reported a highly permeable NF membrane by assembling multi-walled CNTs with rGO (G-CNTm). The permeability of resulting hybridized membrane (11.3 L (m^2 h bar)$^{-1}$) was more than two times higher than that of the corresponding rGO membrane, which can be attributed to the expanded interlayer spacing by CNTs. In addition to the enhanced water permeation, the membrane also showed high rejection for organic contaminants, with >99% for Direct Yellow and >96% for methyl orange (MO). G-CNTm also exhibited good rejection for salts (83.5% for Na_2SO_4) and excellent antifouling performance for sodium alginate (SA) and HA.[51] Gao et al.[52] also blended single-walled carbon nanotubes (SWCNTs) and GO by sonication and prepared SWCNT-intercalated GO ultrathin laminar films by vacuum-filtering on AAO membrane.

Size of the nano-channels of the SWCNT/GO ultrathin membrane increased due to the intercalation of SWCNTs into the stacked GO layers, resulting in an improved water permeability. Permeability increased to 720 ± 50 L $(m^2 h bar)^{-1}$ with a slight decrease in the rejection rate of Coomassie Brilliant Blue dye, when the mass ratio of CNT to GO is 1:4. Instead of physically assembling CNT with rGO, Nellore et al.[43] fabricated a 3D porous membrane by bridging GO and CNTs together with amide bonds; with further peptides modification, the 3D GO hybrid membrane presented antimicrobial and heavy-metal ion retention properties. They demonstrated PGLa modified membrane not only gave 100% rejection for E. coli, but also showed efficient disinfection abilities. Moreover, glutathione attached 3D membrane effectively captured As(III) (98%), As(V) (94%), and Pb(II) (98%) from wastewater.

TiO_2, as a particularly appealing candidate owing to its low cost, high hydrophilicity, and good reactivity with the oxygenated functional groups in GO, was also studied as an effective additive to GO membranes. Fu et al.[53] reported that by assembling TiO_2 nanoparticles with GO, a membrane with an average pore size of ≈3.5 nm can be fabricated. The final GO composite membrane showed relatively high water permeability (7 L $(m^2 h bar)^{-1}$) and almost 100% rejection of MO. Crumpled GO nanocomposite membranes were reported by Jiang et al.;[54] upon assembling these nanocomposites, the resulting membranes achieved extraordinarily high permeability of 246 L $(m^2 h bar)^{-1}$. Moreover, multifunctional membranes were also demonstrated in their work by encapsulating different nanoparticles into GO. GO-TiO_2 nanocomposite based membrane not only presented >80% rejection of bovine serum albumin (BSA) and ≈30% rejection of MO, but also demonstrated in situ photocatalytic degradation ability for MO. GO-Ag nanocomposite based membrane exhibited superior antimicrobial properties. Xu et al.[55] synthesized photocatalytic GO-based hierarchical membranes for water purification by employing TiO_2 decorated GO as separation layer covered by an additional TiO_2 particle layer with strong photocatalytic activity. Superior separation performance resulting from the nano-channels in GO layer as well as the photocatalytic antifouling function provided by TiO_2 nanoparticles (foulant decomposition under UV irradiation) were obtained simultaneously. To prevent the swelling of hydrated GO membranes, monolayer titania (TO)[22,56] flakes were inserted between GO flakes, and then the composite membrane was cross-linked by chitosan (CTS) chains to adjust the interlayer spacing. The rejection of NaCl by GO/TO composite membrane increased greatly from 5% to more than 30% with water flux around 710 L $(m^2 h bar)^{-1}$ which is 70 times more than commercial NF membranes.

Other GO-based nanocomposites incorporated with inorganic nanoparticles can also be a potential candidate for post membrane surface functionalization to derive a synergic effect. Sun et al.[57] developed a GO-AgNPs modified CA membrane by vacuum filtration. The modified membrane showed an inactivation of 86% E. coli, revealing its high antibacterial activity. Photocatalytic performance of the modified membranes were also studied to impede biofouling and prolong the membrane service time.[57]

GO, decorated by TiO_2 as GO-TiO_2 hybrid nanoparticles, has been selected as an efficient photocatalyst for photocatalytic membrane fabrication owing to its outstanding antifouling property.[58] It was reported that addition of GO into TiO_2 matrix increased light absorption in the visible spectral range according to the band-gap energy decrease, which is in agreement with most of the studies on GO-TiO_2 catalyst.[59–67] Three different GO-TiO_2 composite membranes were fabricated by liquid phase deposition (LPD), vacuum filtration and dip-coating methods, respectively.[68–70] Researchers observed the water permeability increase and comparable efficiency of pollutant abatement, when the membrane was exposed to irradiation (UV or visible). This was attributed to the high photocatalytic activity, photo-enhanced hydrophilicity, and antifouling properties along with the GO-TiO_2 modified membrane. Gao et al.[71] grafted the polysulfone (PSF) membrane surface with GO-TiO_2 nanocomposites by a facile deposition method, and conducted both batch and filtration experiments to examine the photocatalytic antifouling property using MB as a contaminant. With the presence of either UV or sunlight irradiation, the modified membrane showed effective and very similar MB photo degradation performance, resulting in efficient removal of the foulant.

SiO_2 was also used to hybridize with GO to form composite membranes. A SiO_2-GO composite membrane was made by seeding and condensing the hydrolysis products of tetraethyl orthosilicate onto the GO sheets.[72] The negatively charged SiO_2-GO composite membrane was used for removing neutral organic molecules (glucose and sucrose), and the best obtained performance was approximately 90% rejection of glucose with water flux around 10 L $(m^2 h bar)^{-1}$.

3.2. Polymer-GO MMM

GO was also used as an effective additive to polymeric membranes to form MMM with improved water separation performance. To date, numerous studies reported the preparation of polymer-GO MMM, such as GO/ PVDF,[73–75] GO/PES[76–78] and GO/PSF[79–81] membranes. The studied polymer-GO MMM showed enhanced hydrophilicity, stability, antifouling, and antibacterial properties due to the outstanding properties of GO. The phase-inversion method was commonly employed for preparing polymer-GO MMM. Normally, a low concentration of GO (<3 wt.%) was dispersed in an organic solvent by sonication to generate a homogeneous solution. Then, pre-dried PVDF, PSF or PES polymer was dissolved in the dope solution. After being fully degassed, the solution was casted on a glass plate, followed by immersion in water bath.[76,79,82]

Compared with the pristine polymer membranes, polymer-GO MMM usually showed structure, porosity, and pore size changes, and exhibited enhanced surface hydrophilicity, which improved the water permeability and membrane antifouling property. **Table 2** summarized polymer-GO MMM for water purification, especially by UF. Zhao et al.[74,75] prepared PVDF-GO MMM with finger-like pore structure along with the increased porosity and pore size. High permeability recovery ratio and low flux decay rate were found, which reflects better antifouling performance resulting from the enhanced hydrophilicity. Zinadini et al.[76,83] fabricated PES-GO MMM by mixing 1 wt.% Polyvinylpyrrolidone (PVP) with GO first

Table 2. Polymer-GO MMM for water purification by UF.

Polymer matrix	GO concentration (wt%)	Water permeability, L (m^2 h bar)$^{-1}$, (Pristine/MMM)	Contaminant rejection (Pristine/MMM)	Main Finding	Reference
PVDF	0.1-0.4	200/800	Kaolin: 99.9%/99.9%	The fabricated PVDF membrane with GO showed a high rejection of Kaolin with outstanding water flux.	[73]
PVDF	0.5-2.0	14.8/26.5	N/A	GO nanosheets penetrate into the finger-like voids and thin-walled sponge pore; increased hydrophilicity leads to higher flux.	[74]
PVP-PVDF	1.0-3.0	(N/A)/443	N/A	Optimum GO concentration on the membrane permeability, antifouling and mechanical properties was found.	[75]
PES	0.1-1.0	2.1/5.1	Dye: 90%/99%	Adding GO flakes to PES membrane led to high rejection of Direct Red 16.	[76]
PES	0.5-1.0	14/20.3	N/A	GO/PES membrane showed anti-fouling property for MBR application.	[83]
PES	0.5-1.0	5.1/9.6	Melanoidin: 44%/59%; Spent wash effluents: 39%/54%	Modified GO with polyacrylic acid showed higher hydrophilicity and thus higher water flux.	[78]
PSF	0.2-2.0	4.9/12.5	Arsenic: 25.9%/83.7%	Adding GO to PSF membrane enhanced the membrane hydrophilicity, porosity, flux and arsenate rejection.	[79]
PSF	0.02-0.39	200/430	N/A	Membrane with GO nano-platelets showed better anti-biofouling capability, superior mechanical strength and water flux.	[80]
PSF	2000 ppm	(N/A)/50	Na_2SO_4: 38%/72%	GO doping into polymer matrix resulted in enhanced hydrophilicity, water flux, and salt rejection. GO was also found to play a major role on modifying membrane morphology.	[81]
PVP-PEI	0.025-0.200	N/A	BSA: 99%/98%	These MMMs demonstrated an improved biocompatibility: reduced protein adsorption, suppressed platelet adhesion, and lower complement activation.	[84]
PDAAQ-PVDF[a)]	0.5-2.0	17.6/68	BSA: 74%/77%	Conductive poly 1,5-diaminoanthraquinone/rGO nanohybrid blended PVDF membrane showed excellent fouling recover by applying very low voltage on membrane.	[44]
APTS-PVDF	0.5-2.0	235/401	BSA: 40%/55%	Organosilane-functionalized GO showed remarkable anti-fouling property and high water flux.	[85]
PSF[b)]	0.1-1.0	8/14	BSA: 92%/89%	Mixture of GO with nano silver particles improved hydrophilicity and permeability, and exhibited superior antibacterial properties.	[86]
PSF[c)]	0.17-0.70	105/135	HA: 81%/98.7%	Adding TiO_2 to GO improved membrane's water flux and anti-fouling properties in removal of humic acid.	[87]
PVDF[d)]	1.0	116.5/410	N/A	Adding oxidized CNTs and GO resulted in higher permeability and anti-fouling performance.	[88]

[a)]reduced GO was added; [b)]GO and Ag nanoparticles were added; [c)]GO and TiO_2 nanoparticles were added; [d)]GO and oxidized CNTs were added; NA = not available. *: relative to the polymer matrix.

and then blended with PES, forming wider finger-like pores. PES-GO (0.5 wt.%) sample showed a 12° decrease of the water contact angle, a 2.5 times increase of the pure water permeability, and as high as 90.5% permeability recovery ratio, after the membrane was fouled by 8,000 ppm powder milk solution, indicating significantly improved hydrophilicity and antifouling property. Similar results were reported on the water permeability and antifouling property for the PSF-GO MMM fabricated by wet phase inversion method.[79–81] Rezaee et al.[79] found that the modified PSF membrane with 1 wt.% GO had the lowest water contact angle and the maximum porosity, pore size and permeability, as well as increased arsenate rejection from 25.9%

for pristine PSF to 83.7%. Lee et al.[80] revealed the anti-biofouling activity of the PSF-GO membrane. They found microorganism amount on the membrane surface decreased with the increase of GO content measured by confocal laser scanning microscopy (CLSM). This may result from the increased negative zeta potential, which induces strong electrostatic repulsion between the microorganism and the membrane surface.

Polymer functionalized GO or GO-polymer co-additives were prepared to improve dispersibility of GO in organic solvents and reinforce interfacial interactions required between GO and the polymer matrix.[89] Kaleekkal et al.[84] incorporated GO-PVP nanocomposite into the poly(ether imide) (PEI) matrix to prepare MMM. They found that the GO-PVP-PEI membrane showed a 4-time increase of the water permeability in UF and improved permeability recovery ratio during the protein filtration. In addition, the GO-PVP-PEI MMM exhibited greater protein adsorption resistance, suppressed platelet adhesion, and prolonged clotting time as compared to the pristine PEI membrane, demonstrating its greater biocompatibility. Yu et al.[90] also modified the GO by hyper-branched PEI and blended into PES solution to prepare MMM, and the high permeability recovery ratio and bacteriostatic rate showed effective antifouling and antibacterial properties. Meanwhile, other polymer or chemically functionalized GO was also reported to illustrate their unique property. Liu et al.[44] prepared a conductive and hydrophilic PVDF membrane with poly(1,5-diaminoanthraquinone)/reduced GO additive. It showed electrocatalytic activity towards oxygen reduction reaction under electric field as well as antifouling ability in BSA filtration. Xu et al.[85] synthesized functionalized GO (f-GO) using 3-aminopropyltriethoxysilane (APTS) and dispersed it into PVDF to form MMM via the phase inversion. Membrane performance, both permeability and BSA rejection, improved by adding GO and f-GO into PVDF. Compared with PVDF-GO membrane, PVDF-f-GO and membrane showed increased water permeability from 160 to 190 L $(m^2\ h\ bar)^{-1}$ and slightly increased BSA rejection from 52 to 58%.

Various inorganic nanoparticles, such as Au,[91] silica,[92] Ag,[86] ZnO,[93] cobalt oxide,[46] and TiO_2,[87] were conjugated on the GO surface to form GO nanoparticle composites. They were mixed with polymers as co-functional additives to prepare UF MMM so the benefits of two types of particles could be combined to exhibit synergistic properties. Mahmoudi et al.[86] decorated GO with Ag nanoparticles and then mixed with PSF to prepare MMM by wet-phase inversion method. Membrane hydrophilicity, solute rejection, permeability and antibacterial properties were all improved with the presence of Ag-GO nanoplates in the membrane matrix. Kumar et al.[87] blended GO with TiO_2 as nano-fillers to synthesize antifouling PSF membranes for HA removal. Both of them reported a higher water permeability and improved antifouling performance of the modified membranes. Additionally, other graphene derivatives, such as CNTs, together with GO have also been investigated as additives for polymeric MMM preparation. Zhang et al.[88] fabricated PVDF MMM with GO/oxidized CNTs as additive to obtain a strong synergetic effect. Due to the co-supporting network of both fillers,[94] excellent dispersion as well as exceptional antifouling and permeability performance was obtained.

GO was also used as effective additive in conventional polymeric membranes to improve their PV performance for water removal from alcohols. **Table 3** summarizes the PV performance of representative polymer-GO MMM for water/alcohol mixtures. Dharupaneedi et al.[95] embedded modified-GO sheets in chitosan polymeric matrix for dehydration of alcohol solvents. Results showed that H-bonding between polar groups and electrostatic interaction between GO and chitons created a good interface, thereby improving permeability, thermal and physic-mechanical characteristics. GO flakes also decreased alcohol affinity while increasing water affinity, which significantly increased diffusion resistance for alcohols. Cao et al.[96] added rGO and GO in SA and studied ethanol/water separation by PV. They found that the resulting MMM exhibited unusual crystallinity change and had increased free volume. MMM with rGO additive had the highest separation factor and permeability because of the synergy between permselectivity of water channels and crystallinity of polymer matrix. Moreover, due to the interfacial interaction between rGO nanosheets and SA chains, the MMM had high swelling resistance and mechanical stability.[97] Sulfonated poly ether sulfone (SPES) membrane with sulfonated GO additive showed similar behavior as that of SA/rGO MMM. Gahlot et al.[98] reported that adding sulfonated GO to SPES matrix increased permeability as well as thermal and physical properties. Generally, comparison between GO-based membranes with lamellar structure and polymer-GO MMM in PV (Tables 1 and 3) shows that former usually has higher flux than latter, while physical- mechanical and thermal properties of polymer-GO MMM are typically better than GO-based membranes.

Thin film composite (TFC) membranes usually have high water permeability and good separation factor because of the thin active layer thickness, typically less than 300 nm. Recently, adding nanoparticles in this layer creates a new type of high performance membrane for water desalination.[49,101,102] In GO-TFC MMM preparation, GO flakes were blended into polymer matrix during interfacial polymerization reaction to

Table 3. PV performance of polymer-GO mix MMM for water/alcohol mixtures.

Alcohol	Polymeric Matrix	Separation condition	Flux, g m^{-2} h^{-1}	Separation factor	Reference
Ethanol (Eth), Isopropanol (IPA), Isobutanol (IBA)	PEI+PAA	t: 50 °C Water: 5%	Eth = 196 IPA = 210 IBA = 215	Eth = 600 IPA = 650 IBA = 680	[99]
Ethanol	SA	t: 30 to 60 °C Water: 10%	550	4,623	[100]
Ethanol	SA	t: 40 to 70 °C Water: 10%	1,699	1566	[96]
Ethanol (Eth) and Isopropanol (IPA)	Chitson	t: 40 to 60 °C water: 10%	Eth = 250 IPA = 310	Eth = 1093 IPA = 7711	[95]
Ethanol	SPES	t: ≈25 °C Water: 30%	910	28	[98]

improve the physical properties of the host polymers.[45,103–107] By directly involving GO flakes into interfacial polymerization, Bano et al.[104] reported the fabrication of novel polyamide (PA)-GO MMM. Unlike physically blending GO with polymer, GO flakes cross-linked with TMC via the formation of ester bonds during the polymerization process. Upon GO loading from 0.0 to 0.3%, the hydrophilicity and zeta potential of the membrane increased, and the surface roughness decreased. While maintaining high salt retention, water permeability of PA-GO MMM increased drastically from 0.46 to 1.54 L (m^2 h bar)$^{-1}$, and presented excellent antifouling properties for BSA and HA. Chae et al.[103] reported the fabrication of thin film nanocomposite (TFN) membranes by introducing GO into the polymerization process between m-phenylenediamine (MPD) and TMC to form PA. The resulting membranes (GO-TFC) showed improved hydrophilicity and decreased surface roughness and the zeta potential with the increase of the GO loading. Permeability of the 38-GO-TFC (38 ppm GO content) membrane (1.08 L (m^2 h bar)$^{-1}$) was about 80% higher than that of the TFC membrane. The anti-biofouling property of GO-TFC membranes was evaluated by a cell attachment test; smooth, negatively charged and more hydrophilic surface led to greatly improved membrane antifouling performance. Because of the H-bonding between embedded GO and PA, the salt rejection of GO-TFC was retained at 2,000 ppm NaCl. By applying a similar idea, Safarpour et al.[108] embedded rGO/TiO_2 nanocomposites into PA polymer matrix during polymerization between MPD and TMC. The resulting rGO/TiO_2/RO membrane exhibited 3.42 L (m^2 h bar)$^{-1}$ water permeability and 99.45% salt rejection at rGO/TiO_2 loading of 0.02 wt%. With the incorporation of rGO/TiO_2, the anti-biofouling ability of the rGO/TiO_2/RO membranes was greatly improved; also, salt rejection only dropped 3% upon chlorination.

4. GO Functional Coatings on Membranes

GO was also used as an effective functional coating material for MF, UF, RO membranes to enhance surface-based interactions, for example, to increase permeability during filtration, improve antifouling performance of UF membranes, and enhance chlorine resistance and anti-biofouling properties of RO membranes.[15,109–111] Typically, GO functional coatings on membranes or sometimes on meshes were deposited by dip-coating, vacuum filtration, or chemical bonding on the surface. Hibbs et al.[112] demonstrated, by reacting with 1-ethyl-3-[3-(dimethylamino)propyl] carbodiimide (EDC) and N-hydroxysuccinimide (NHS), followed by cross-linking with EDA, GO can be reversibly bonded to PA RO membrane surface (78.6% coverage). GO surface modification exhibited no detrimental effect on intrinsic PA RO membrane transport properties. Anti-biofouling performance of the resulting membranes, however, was enhanced by reducing about 65% of E. coli on the membrane surface. To improve both antifouling and chlorine resistance of the PA membrane, Chai et al.[113] deposited oppositely charged GO, aminated GO and regular GO on the surface of the PA membrane through LBL method. GO multilayers, therefore, packed tightly on PA surface through electrostatic interaction. Compared with neat PA membrane, ten GO bilayer (GO10) coated PA membrane showed lower surface roughness and improved hydrophilicity. Membrane permeation performance remained almost the same after GO coating. Water permeability of GO10-coated PA membrane, however, reduced only 15% after 12 h filtration of BSA (100 mg L^{-1}) solution. In contrast, permeability of PA membranes decreased linearly from 0.8 to less than 0.53 L/(m^2.h.bar) after 12 h filtration. This demonstrates high anti-biofouling capability and chlorine resistance improvement for PA based RO membrane after GO coating.

GO coatings can also work as a surface modifier to increase water permeability, suppress salt reverse flow, and improve antifouling ability of FO membranes. Ginic-Markovic et al.[114] developed two methods, LbL strategy and hybrid (H)-grafting strategy, to attach GO on the surface of TFC PA FO membrane via poly L-lysine (PLL). After GO/PLL surface modification, water permeability maintained almost the same as the neat PA membrane, whereas the reverse flow (2 M NaCl draw solution) of GO/PLL-H membrane dramatically decreased 63% and that of GO/PLL-LBL membrane increased 78%. This suggested H-grafting of GO was a better way to improve desalination performance of PA based FO membrane. The resulting GO/PLL-H membrane also exhibited high antibacterial activity. By applying a similar idea, Ray et al.[115] sequentially deposited Au nanostars (AuNS) and polyethylene glycol (PEG) to fabricate a novel PA-GO-AuNS-PEG membrane. The resulting membrane not only retained similar performance to the PA membrane, but also reduced fouling from minerals ($CaCO_3$ and $CaSO_4$), organics (HA) and bacteria (E. coli). The mechanism of the multi-antifouling properties of the PA-GO-AuNS-PEG membrane was also investigated. They suggested that the neutral surface charge and Au particles prevented nucleation of Ca^{2+}. Consequently, the mineral scaling of the membrane was prevented. Moreover, attributed to the hydrophilic and uncharged surface properties and AuNS's ability to prevent organic matter accumulation, the PA-GO-AuNS-PEG membrane also exhibited good anti-organic fouling ability.

Soroush et al.[110] recently reported GO/AgNPs decorated TFC/PA/FO membrane with significantly improved anti-biofouling ability. GO flakes worked as a support for anti-bacterial AgNPs, and the GO/AgNPs composite was then grafted on the PA surface using cysteamine via amide bonds. While retaining the membrane transport property, the resulting GO/AgNPs/PA membrane exhibited >95% bacterial inactivation for E. coli. Similar GO/AgNPs/PA membranes were prepared by Asadishad and co-workers.[109] Rather than synthesizing GO/AgNPs composite first, they did Ag decoration in situ on the top of GO modified PA membrane. The resulting GO/AgNPs/PA membrane showed improved bacterial inactivation for E. coli.D21f2, E. coli. O157:H7, and Enterococcus faecalis. Moreover, after 7 days' Ag releasing, surface Ag particles could be regenerated by the same way. After Ag regeneration, membrane could retain its antibacterial properties and 75% of its initial Ag loading.

Hydrophilic GO coatings can also be used to improve the separation performance of polymeric UF membranes and mitigate their fouling problems. Contaminants and pollutants including microorganisms, bacteria, oil, proteins, and even heavy metal ions (e.g., Hg, Cd, and As ions) can be effectively removed from the wastewater by UF. Huang et al.[116] designed and fabricated GO/PA UF membranes with optimized hierarchical surface

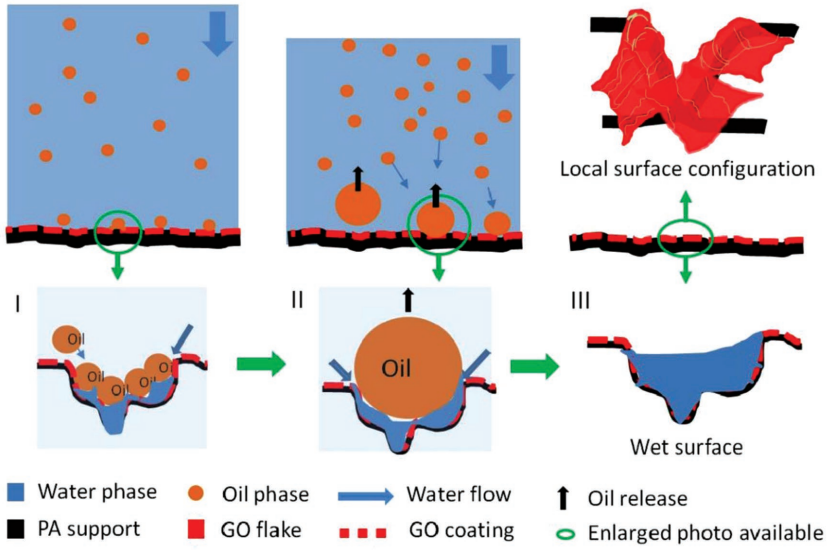

Figure 7. Schematic illustration of underwater antifouling behavior of GO coated PA surface in the process of oil/water emulsion separation: (I) oil droplets in contract with GO coated membrane surface, (II) accumulation of oil droplets and release of big oil droplets, and (III) GO coated PA membrane after water flushing/cleaning. Reproduced with permission.[116]

roughness by facile vacuum filtration for antifouling oil/water separation. They observed full recovery of the pure water permeability with the 10 nm thickness GO coating on the PA membrane surface, indicating absence of surface fouling and minimization of internal fouling in the membrane. Thereafter, Li et al.[117] treated GO dispersion with UV irradiation to modify its surface properties, and prepared 10 nm GO coated PA membranes with tunable underwater oleophobicity. They found a higher percentage of hydrophilic oxygen-containing functional groups on the GO flakes after UV treatment, which led to its underwater superoleophobic property. **Figure 7** shows the proposed anti-fouling mechanism of the GO coated PA membranes in oil/water separation. Musico et al.[118] prepared GO and poly (N-vinylcarbazole)-GO (PVK-GO) functionalized cellulose nitrate (CN) membranes by vacuum filtration, and investigated their anti-bacterial ability using E. coli and Bacillus subtilis (B. subtilis) solution. The membrane pore size decreased after GO and PVK-GO coating, leading to an increase of the rejection for the bacteria. They also found that both GO and PVK-GO plate counts presented a removal of 4 and 3 logs for B. subtilis and E. coli, indicating the improved anti-bacterial capability of GO functionalized membranes. Liu et al.[119] reported a GO coated wire mesh fabricated by drop-coating method for oil/water separation, and they observed superoleophobicity and good durability of the GO-embellished mesh.

GO quantum dots (GOQDs), small GO nanosheets with the diameter in the range of 3–20 nm,[120] have been applied in the antibacterial research field due to their unique properties, such as morphology,[121] ultrasmall lateral sizes,[122] and cytotoxicity[123] etc. However, few studies reported application of GOQDs on membrane fabrication or modification. Zeng et al.[124] employed them for preparing GOQD-functionalized PVDF membrane with bactericidal and anti-biofouling abilities. Modified GOQD-PVDF membrane showed significantly improved hydrophilic, anti-bacterial and anti-biofouling properties without sacrificing the permeation property of the pristine PVDF membrane. Modified GOQD-PVDF membrane was even superior to GO-PVDF membrane.

5. Separation Stability and Thermal/Mechanical Properties

Table 4 summarizes the separation stability and thermal/mechanical properties of different types of GO-related membranes. The performance stability of membranes with GO as the selective layer (type I) was studied for water/alcohol PV separation from 30 to 1800 h.[30,32,36] Tang et al.[32] compared mechanical properties of free-standing GO membranes with PS membrane, and found that GO membranes had improved Young's modulus and tensile stress. The separation stability of was investigated by Chen et al.[30] The separation factor and flux were almost stable in the temperature range of 25 to 80 °C, after running for about 30 h.

Table 4. Separation stability and thermal/mechanical properties of GO-related membranes.

Membrane type*	Application	Separation stability	Thermal/mechanical properties	Reference
I	PV	30 to 1600 h testing with negligible performance change	higher tensile and better thermal stability than dense PSF membrane.	[30,32,36]
II	UF	Stable upon chemical washing at different pH	Improvement of thermal stability, tensile strength and elongation	[73,125–127]
	RO	Constant performance of PA/GO in 5 h.	–	[104,106]
	PV	Stable operation from 5 to 144 h	Slight improvement of degradation temperature, Young's modulus and hardness	[28,95,96,99]
III	UF	Almost stable performance of E. coli separation for 20 h.	–	[124]
	RO	Stable under E. coli separation for 6 h.	–	[109]

*: As defined in Figure 4.

The separation stability and thermal/mechanical properties of GO-MMM membranes (type II) are similar to those of the polymer matrix.[28,95,96,99] Typically, GO sheets as additive improved mechanical properties, such as Young's modules, elongation, and hardness as well as thermal stability. Permeation results of GO/EDA MMM membrane showed that water flux and water/alcohol separation factor changed during the first several hours and then reached steady state and kept constant for over more than 144 h.[28] GO sheets in polymeric UF membranes also enhanced separation stability under chemical washing and at different pH values as well as mechanical properties.[73,125–127] However, limited studies have been focused on performance stability and mechanical/thermal properties of GO-MMM membrane for RO and NF membrane.[104,106]

The performance stability of GO functional coatings (type III) was studied for only several hours for E. coli separation,[124] and there is no study on thermal/mechanical stability of those coated GO and long-term performance stability.

6. Conclusions and Outlook

Significant progress has been made on using 2-D GO as a novel material in membrane separation for water purification, from PV, RO, NF to UF and MF. 2-D, hydrophilic nano-channels of GO-based membranes with lamellar structure have shown great potential for highly selectively extracting water from organics by PV and removing >≈1 nm organic molecules and partially removing ions by NF. Fundamental understanding on interlayer nanostructures and how to effectively control and design them for targeted separation are still missing. Membrane stability over long operation time and in different feed conditions is a potential concern, although various molecular linkers have been used to interconnect adjacent GO flakes together and sometimes chemical bonding between GO and substrates were also formed. In addition, GO-based membranes with lamellar structure are still too thick (typically >10 nm), which usually corresponds to longer than 1 μm transport pathway. Therefore, effective and scalable GO coating processes need to be developed to deposit thinner (<5 nm) layers composed of smaller GO flakes that are packed uniformly in lamellar structure. Effective techniques are also needed to stabilize ultrathin GO-based membranes. GO, as a novel additive for MMM, can greatly improve the membrane surface hydrophilicity, create additional pathway for water molecules through the membrane matrix, and increase mechanical strength of the membrane matrix. As a result, MMM with GO additive, at the optimum GO loading, usually showed improved water separation performance. However, understanding of interactions between polymers or GO at the interface, dispersing GO uniformly in organic solvents, and developing effective coating methods and post-treatment methods to minimize defects of MMM are still challenging. GO or modified GO functional coatings have been shown to significantly improve the antifouling/anti-bacterial properties of RO and UF membranes. Functional coatings with only several layers of GO/modified GO effectively covered membranes surface but had negligible resistance for water transport. These novel and ultrathin (<5 nm) functional coatings may have wide applications on improving antifouling/anti-bacterial resistance

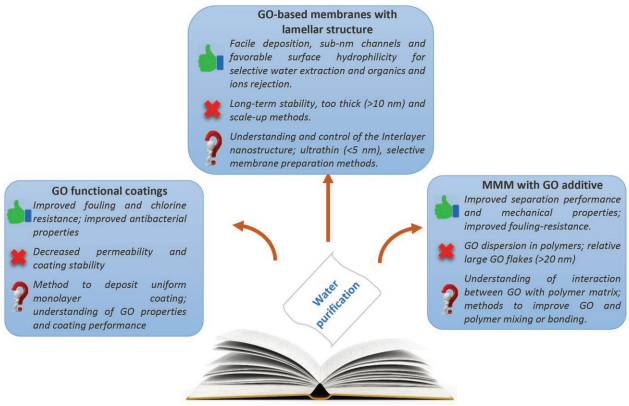

Figure 8. Outlook of GO-incorporated membranes for water purification.

of commercial membranes, although coating stability over long time operation may be a potential concern. **Figure 8** shows the outlook of GO-incorporated membranes for water purification. In conclusion, GO, as a novel 2-D material with sub-nanometer thickness, high lateral size to thickness ratio, excellent flexibility and thus good conformality to the substrates with various morphology, rich oxygen-containing functional groups, and good compatibility with various materials, allows very flexible use in membrane configuration and is expected to have wide applications in membrane separation for water purification.

Acknowledgements

M.F., W.L.X., and F.Z. contributed equally to this work. We gratefully acknowledge the support by National Science Foundation (NSF) Career Award under Grant No. 1451887.

Received: September 23, 2016
Revised: November 19, 2016
Published online:

[1] W. S. Hummers, R. E. Offeman, *J. Am. Chem. Soc.* **1958**, *80*, 1339.
[2] J. R. Lomeda, C. D. Doyle, D. V. Kosynkin, W. F. Hwang, J. M. Tour, *J. Am. Chem. Soc.* **2008**, *130*, 16201.
[3] Q. Xu, H. Xu, J. R. Chen, Y. Z. Lv, C. B. Dong, T. S. Sreeprasad, *Inorg. Chem. Front.* **2015**, *2*, 417.
[4] H. M. Hegab, L. D. Zou, *J. Membr. Sci.* **2015**, *484*, 95.
[5] D. Cohen-Tanugi, J. C. Grossman, *Nano Lett.* **2012**, *12*, 3602.
[6] L. C. Lin, J. C. Grossman, *Nat. Commun.* **2015**, *6*.
[7] D. Konatham, J. Yu, T. A. Ho, A. Striolo, *Langmuir* **2013**, *29*, 11884.
[8] S. P. Surwade, S. N. Smirnov, I. V. Vlassiouk, R. R. Unocic, G. M. Veith, S. Dai, S. M. Mahurin, *Nat. Nanotechnol.* **2015**, *10*, 459.
[9] S. C. O'Hern, M. S. H. Boutilier, J. C. Idrobo, Y. Song, J. Kong, T. Laoui, M. Atieh, R. Karnik, *Nano Lett.* **2014**, *14*, 1234.
[10] H. P. Boehm, A. Clauss, U. Hofmann, *J. Chim. Phys. PCB* **1961**, *58*, 141.
[11] E. S. Bober, U. S. O. o. S. Water, W. E. Corporation, *Final Report On Reverse Osmosis Membranes Containing Graphitic Oxide*, U.S. Dept. of the Interior, **1970**.
[12] R. R. Nair, H. A. Wu, P. N. Jayaram, I. V. Grigorieva, A. K. Geim, *Science* **2012**, *335*, 442.

[13] R. K. Joshi, P. Carbone, F. C. Wang, V. G. Kravets, Y. Su, I. V. Grigorieva, H. A. Wu, A. K. Geim, R. R. Nair, *Science* **2014**, *343*, 752.
[14] N. Wei, X. S. Peng, Z. P. Xu, *Acs Appl. Mater. Inter.* **2014**, *6*, 5877.
[15] H. Li, Z. N. Song, X. J. Zhang, Y. Huang, S. G. Li, Y. T. Mao, H. J. Ploehn, Y. Bao, M. Yu, *Science* **2013**, *342*, 95.
[16] X. L. Qu, P. J. J. Alvarez, Q. L. Li, *Water Res.* **2013**, *47*, 3931.
[17] K. A. Mahmoud, B. Mansoor, A. Mansour, M. Khraisheh, *Desalination* **2015**, *356*, 208.
[18] L. Wang, N. X. Wang, J. Li, J. W. Li, W. W. Bian, S. L. Ji, *Sep. Purif. Technol.* **2016**, *160*, 123.
[19] M. Hu, B. X. Mi, *Environ. Sci. Technol.* **2013**, *47*, 3715.
[20] P. Z. Sun, M. Zhu, K. L. Wang, M. L. Zhong, J. Q. Wei, D. H. Wu, Z. P. Xu, H. W. Zhu, *ACS Nano* **2013**, *7*, 428.
[21] H. B. Huang, Y. Y. Mao, Y. L. Ying, Y. Liu, L. W. Sun, X. S. Peng, *Chem. Commun.* **2013**, *49*, 5963.
[22] H. Deng, P. Z. Sun, Y. J. Zhang, H. W. Zhu, *Nanotechnology* **2016**, *27*.
[23] Y. Han, Z. Xu, C. Gao, *Adv. Funct. Mater.* **2013**, *23*, 3693.
[24] H. Y. Liu, H. T. Wang, X. W. Zhang, *Adv. Mater.* **2015**, *27*, 249.
[25] J. J. Song, Y. Huang, S. W. Nam, M. Yu, J. Heo, N. Her, J. R. V. Flora, Y. Yoon, *Sep. Purif. Technol.* **2015**, *144*, 162.
[26] R. Liu, G. Arabale, J. Kim, K. Sun, Y. Lee, C. Ryu, C. Lee, *Carbon* **2014**, *77*, 933.
[27] K. Huang, G. P. Liu, Y. Y. Lou, Z. Y. Dong, J. Shen, W. Q. Jin, *Angew. Chem. Int. Ed.* **2014**, *53*, 6929.
[28] G. H. Li, L. Shi, G. F. Zeng, Y. F. Zhang, Y. H. Sun, *RSC Adv.* **2014**, *4*, 52012.
[29] C. H. Tsou, Q. F. An, S. C. Lo, M. De Guzman, W. S. Hung, C. C. Hu, K. R. Lee, J. Y. Lai, *J. Membr. Sci.* **2015**, *477*, 93.
[30] X. F. Chen, G. P. Liu, H. Y. Zhang, Y. Q. Fan, *Chinese J. Chem. Eng.* **2015**, *23*, 1102.
[31] M. Paulauskas, M. Frans, "Separation of Water and Isopropyl Alohol Mixtures with Graphene Oxide Membranes", presented at *the 2nd International Conference on Fluid Flow, Heat and Mass Transfer*, Ottawa, Ontario, Canada, April 30-May 1, **2015**.
[32] Y. P. Tang, D. R. Paul, T. S. Chung, *J. Membr. Sci.* **2014**, *458*, 199.
[33] W. S. Hung, Q. F. An, M. De Guzman, H. Y. Lin, S. H. Huang, W. R. Liu, C. C. Hu, K. R. Lee, J. Y. Lai, *Carbon* **2014**, *68*, 670.
[34] T. M. Yeh, Z. Wang, D. Mahajan, B. S. Hsiao, B. Chu, *J. Mater. Chem. A* **2013**, *1*, 12998.
[35] W. S. Hung, C. H. Tsou, M. De Guzman, Q. F. An, Y. L. Liu, Y. M. Zhang, C. C. Hu, K. R. Lee, J. Y. Lai, *Chem. Mater.* **2014**, *26*, 2983.
[36] G. H. Li, L. Shi, G. F. Zeng, M. Li, Y. F. Zhang, Y. H. Sun, *Chem. Commun.* **2015**, *51*, 7345.
[37] C. N. Yeh, K. Raidongia, J. J. Shao, Q. H. Yang, J. X. Huang, *Nat. Chem.* **2015**, *7*, 166.
[38] Y. Zhang, S. Zhang, T. S. Chung, *Environ. Sci. Technol.* **2015**, *49*, 10235.
[39] S. J. Xia, M. Ni, T. R. Zhu, Y. Zhao, N. N. Li, *Desalination* **2015**, *371*, 78.
[40] A. K. Mishra, S. Ramaprabhu, *Desalination* **2011**, *282*, 39.
[41] J. Y. Chong, N. F. D. Aba, B. Wang, C. Mattevi, K. Li, *Sci. Rep.* **2015**, *5*. doi: 10.1038/srep15799.
[42] X. F. Chen, M. H. Qiu, H. Ding, K. Y. Fu, Y. Q. Fan, *Nanoscale* **2016**, *8*, 5696.
[43] B. P. V. Nellore, R. Kanchanapally, F. Pedraza, S. S. Sinha, A. Pramanik, A. T. Hamme, Z. Arslan, D. Sardar, P. C. Ray, *ACS Appl. Mater. Inter.* **2015**, *7*, 19210.
[44] H. Y. Liu, G. Q. Zhang, C. Q. Zhao, J. D. Liu, F. L. Yang, *J. Mater. Chem. A* **2015**, *3*, 20277.
[45] S. Inukai, R. Cruz-Silva, J. Ortiz-Medina, A. Morelos-Gomez, K. Takeuchi, T. Hayashi, A. Tanioka, T. Araki, S. Tejima, T. Noguchi, M. Terrones, M. Endo, *Sci. Rep.* **2015**, *5*. doi: 10.1038/srep13562.
[46] G. Ouyang, A. Hussain, J. B. Li, D. X. Li, *RSC Adv.* **2015**, *5*, 70448.
[47] H. Q. Wu, B. B. Tang, P. Y. Wu, *J. Membr. Sci.* **2014**, *451*, 94.
[48] N. J. Kaleekkal, A. Thanigaivelan, M. Durga, R. Girish, D. Rana, P. Soundararajan, D. Mohan, *Ind. Eng. Chem. Res.* **2015**, *54*, 7899.
[49] M. Fathizadeh, A. Aroujalian, A. Raisi, *J. Membr. Sci.* **2011**, *375*, 88.
[50] M. Fathizadeh, A. Aroujalian, A. Raisi, *Desalination* **2012**, *284*, 32.
[51] Y. Han, Y. Q. Jiang, C. Gao, *Acs Appl. Mater. Inter.* **2015**, *7*, 8147.
[52] S. J. Gao, H. L. Qin, P. P. Liu, J. Jin, *J. Mater. Chem. A* **2015**, *3*, 6649.
[53] C. Xu, A. J. Cui, Y. L. Xu, X. Z. Fu, *Carbon* **2013**, *62*, 465.
[54] Y. Jiang, D. Liu, M. J. Cho, S. S. Lee, F. Z. Zhang, P. Biswas, J. D. Fortner, *Environ. Sci. Technol.* **2016**, *50*, 2514.
[55] C. Xu, Y. L. Xu, J. L. Zhu, *ACS Appl. Mater. Inter.* **2014**, *6*, 16117.
[56] Pengzhan Sun, Qiao Chen, Xinda Li, He Liu, Kunlin Wang, Minlin Zhong, Jinquan Wei, Renzhi Ma, Takayoshi Sasaki, Hongwei Zhu, D. Wu, *NPG Asia Mater.* **2015**, *7*, 8.
[57] X. F. Sun, J. Qin, P. F. Xia, B. B. Guo, C. M. Yang, C. Song, S. G. Wang, *Chem. Eng. J.* **2015**, *281*, 53.
[58] M. C. Long, Y. L. Qin, C. Chen, X. Y. Guo, B. H. Tan, W. M. Cai, *J. Phys. Chem. C* **2013**, *117*, 16734.
[59] D. L. Zhao, G. D. Sheng, C. L. Chen, X. K. Wang, *Appl. Catal. B-Environ.* **2012**, *111*, 303.
[60] M. S. A. S. Shah, A. R. Park, K. Zhang, J. H. Park, P. J. Yoo, *ACS Appl. Mater. Inter.* **2012**, *4*, 3893.
[61] Y. L. Min, K. Zhang, W. Zhao, F. C. Zheng, Y. C. Chen, Y. G. Zhang, *Chem. Eng. J.* **2012**, *193*, 203.
[62] H. B. Li, W. Zhang, L. D. Zou, L. K. Pan, Z. Sun, *J. Mater. Res.* **2011**, *26*, 970.
[63] Y. P. Zhang, C. X. Pan, *J. Mater. Sci.* **2011**, *46*, 2622.
[64] J. C. Liu, H. W. Bai, Y. J. Wang, Z. Y. Liu, X. W. Zhang, D. D. Sun, *Adv. Funct. Mater.* **2010**, *20*, 4175.
[65] R. M. Mohamed, *Desalin. Water. Treat.* **2012**, *50*, 147.
[66] G. D. Jiang, Z. F. Lin, C. Chen, L. H. Zhu, Q. Chang, N. Wang, W. Wei, H. Q. Tang, *Carbon* **2011**, *49*, 2693.
[67] D. H. Yoo, V. C. Tran, V. H. Pham, J. S. Chung, N. T. Khoa, E. J. Kim, S. H. Hahn, *Curr. Appl. Phys.* **2011**, *11*, 805.
[68] C. P. Athanasekou, S. Morales-Torres, V. Likodimos, G. E. Romanos, L. M. Pastrana-Martinez, P. Falaras, D. D. Dionysiou, J. L. Faria, J. L. Figueiredo, A. M. T. Silva, *Appl. Catal. B-Environ.* **2014**, *158*, 361.
[69] C. P. Athanasekou, N. G. Moustakas, S. Morales-Torres, L. M. Pastrana-Martinez, J. L. Figueiredob, J. L. Faria, A. M. T. Silva, J. M. Dona-Rodriguez, G. E. M. Romanos, P. Falaras, *Appl. Catal. B-Environ.* **2015**, *178*, 12.
[70] L. M. Pastrana-Martinez, S. Morales-Torres, J. L. Figueiredo, J. L. Faria, A. M. T. Silva, *Water Res.* **2015**, *77*, 179.
[71] Y. Gao, M. Hu, B. X. Mi, *J. Membr. Sci.* **2014**, *455*, 349.
[72] S. X. Zheng, B. X. Mi, *Environ Sci-Wat Res* **2016**, *2*, 717.
[73] W. Jang, J. Yun, K. Jeon, H. Byun, *RSC Advances* **2015**, *5*, 46711.
[74] C. Zhao, X. Xu, J. Chen, F. Yang, *J. Environ. Chem. Eng.* **2013**, *1*, 349.
[75] C. Zhao, X. Xu, J. Chen, F. Yang, *Desalination* **2014**, *334*, 17.
[76] S. Zinadini, A. A. Zinatizadeh, M. Rahimi, V. Vatanpour, H. Zangeneh, *J. Membr. Sci.* **2014**, *453*, 292.
[77] S. Zinadini, V. Vatanpour, A. A. Zinatizadeh, M. Rahimi, K. M. , *J. Water Process Eng.* **2015**, *7*, 280.
[78] S. A. Kiran, Y. L. Thuyavan, G. Arthanareeswaran, T. Matsuura, A. Ismail, *Chem. Eng. J.* **2016**, *286*, 528.
[79] R. Rezaee, S. Nasseri, A. H. Mahvi, R. Nabizadeh, S. A. Mousavi, A. Rashidi, A. Jafari, S. Nazmara, *J. Environ. Health. Sci.* **2015**, *13*, 179.

[80] J. Lee, H.-R. Chae, Y. J. Won, K. Lee, C.-H. Lee, H. H. Lee, I.-C. Kim, J.-m. Lee, *J. Membr. Sci.* **2013**, *448*, 223.
[81] B. Ganesh, A. M. Isloor, A. F. Ismail, *Desalination* **2013**, *313*, 199.
[82] C. Q. Zhao, X. C. Xu, J. Chen, F. L. Yang, *Desalination* **2014**, *334*, 17.
[83] S. Zinadini, V. Vatanpour, A. A. Zinatizadeh, M. Rahimi, Z. Rahimi, M. Kian, *J. Water Process Eng.* **2015**, *7*, 280.
[84] N. J. Kaleekkal, A. Thanigaivelan, M. Durga, R. Girish, D. Rana, P. Soundararajan, D. Mohan, *Ind. Eng. Chem. Res.* **2015**, *54*, 7899.
[85] Z. Xu, J. Zhang, M. Shan, Y. Li, B. Li, J. Niu, B. Zhou, X. Qian, *J. Membr. Sci.* **2014**, *458*, 1.
[86] E. Mahmoudi, L. Y. Ng, M. M. Ba-Abbad, A. W. Mohammad, *Chem. Eng. J.* **2015**, *277*, 1.
[87] M. Kumar, Z. Gholamvand, A. Morrissey, K. Nolan, M. Ulbricht, J. Lawler, *J. Membr. Sci.* **2016**, *506*, 38.
[88] J. Zhang, Z. Xu, M. Shan, B. Zhou, Y. Li, B. Li, J. Niu, X. Qian, *J. Membr. Sci.* **2013**, *448*, 81.
[89] H. F. Yang, F. H. Li, C. S. Shan, D. X. Han, Q. X. Zhang, L. Niu, A. Ivaska, *J. Mater. Chem.* **2009**, *19*, 4632.
[90] L. Yu, Y. Zhang, B. Zhang, J. Liu, H. Zhang, C. Song, *J. Membr. Sci.* **2013**, *447*, 452.
[91] G. Goncalves, P. A. Marques, C. M. Granadeiro, H. I. Nogueira, M. Singh, J. Gracio, *Chem. Mater.* **2009**, *21*, 4796.
[92] H. Wu, B. Tang, P. Wu, *J. Membr. Sci.* **2014**, *451*, 94.
[93] G. Williams, P. V. Kamat, *Langmuir* **2009**, *25*, 13869.
[94] S. Chatterjee, F. Nafezarefi, N. Tai, L. Schlagenhauf, F. Nüesch, B. Chu, *Carbon* **2012**, *50*, 5380.
[95] S. P. Dharupaneedi, R. V. Anjanapura, J. M. Han, T. M. Aminabhavi, *Ind. Eng. Chem. Res.* **2014**, *53*, 14474.
[96] K. T. Cao, Z. Y. Jiang, J. Zhao, C. H. Zhao, C. Y. Gao, F. S. Pan, B. Y. Wang, X. Z. Cao, J. Yang, *J. Membr. Sci.* **2014**, *469*, 272.
[97] M. M. Ga, S. C. Georgea, T. Josea, S. Thomas, *J. Membr. Sep. Tech.* **2014**, *3*, 178.
[98] S. Gahlot, P. P. Sharma, B. M. Bhil, H. Gupta, V. Kulshrestha, *Macromol. Symp.* **2015**, *359*, 189.
[99] N. X. Wang, S. L. Ji, G. J. Zhang, J. Li, L. Wang, *Chem. Eng. J.* **2012**, *213*, 318.
[100] D. P. Suhas, A. V. Raghu, H. M. Jeong, T. M. Aminabhavi, *RSC Adv.* **2013**, *3*, 17120.
[101] A. Soroush, J. Barzin, M. Barikani, M. Fathizadeh, *Desalination* **2012**, *287*, 310.
[102] M. Fathizadeh, A. Aroujalian, A. Raisi, *Desalin. Water. Treat.* **2015**, *56*, 2284.
[103] H. R. Chae, J. Lee, C. H. Lee, I. C. Kim, P. K. Park, *J. Membr. Sci.* **2015**, *483*, 128.
[104] S. Bano, A. Mahmood, S. J. Kim, K. H. Lee, *J. Mater. Chem. A* **2015**, *3*, 2065.
[105] S. G. Kim, D. H. Hyeon, J. H. Chun, B. H. Chun, S. H. Kim, *Desalin. Water. Treat.* **2013**, *51*, 6338.
[106] S. J. Xia, L. J. Yao, Y. Zhao, N. N. Li, Y. Zheng, *Chem. Eng. J.* **2015**, *280*, 720.
[107] H. J. Kim, M. Y. Lim, K. H. Jung, D. G. Kim, J. C. Lee, *J. Mater. Chem. A* **2015**, *3*, 6798.
[108] M. Safarpour, A. Khataee, V. Vatanpour, *J. Membr. Sci.* **2015**, *489*, 43.
[109] A. Soroush, W. Ma, M. Cyr, M. S. Rahaman, B. Asadishad, N. Tufenkji, *Environ. Sci. Tech. Let.* **2016**, *3*, 13.
[110] A. Soroush, W. Ma, Y. Silvino, M. S. Rahaman, *Environ. Sci-Nano.* **2015**, *2*, 395.
[111] H. B. Huang, Z. G. Song, N. Wei, L. Shi, Y. Y. Mao, Y. L. Ying, L. W. Sun, Z. P. Xu, X. S. Peng, *Nat. Commun.* **2013**, *4*. doi: 10.1038/ncomms3979.
[112] M. R. Hibbs, L. K. McGrath, S. Kang, A. Adout, S. J. Altman, M. Elimelech, C. J. Cornelius, *Desalination* **2016**, *380*, 52.
[113] W. Choi, J. Choi, J. Bang, J. H. Lee, *Acs Appl. Mater. Inter.* **2013**, *5*, 12510.
[114] H. M. Hegab, A. ElMekawy, T. G. Barclay, A. Michelmore, L. D. Zou, C. P. Saint, M. Ginic-Markovic, *ACS Appl. Mater. Inter.* **2015**, *7*, 18004.
[115] J. R. Ray, S. Tadepalli, S. Z. Nergiz, K. K. Liu, L. You, Y. J. Tang, S. Singamaneni, Y. S. Jun, *ACS Appl. Mater. Inter.* **2015**, *7*, 11117.
[116] Y. Huang, H. Li, L. Wang, Y. L. Qiao, C. B. Tang, C. I. Jung, Y. M. Yoon, S. G. Li, M. Yu, *Adv. Mater. Interfaces.* **2015**, *2*, 1400433.
[117] H. Li, Y. Huang, Y. Mao, W. L. Xu, H. J. Ploehn, M. Yu, *Chem. Commun.* **2014**, *50*, 9849.
[118] Y. L. F. Musico, C. M. Santos, M. L. P. Dalida, D. F. Rodrigues, *ACS Sustain. Chem. Eng.* **2014**, *2*, 1559.
[119] Y. Q. Liu, Y. L. Zhang, X. Y. Fu, H. B. Sun, *ACS Appl. Mater. Interfaces* **2015**, *7*, 20930.
[120] J. Shen, Y. Zhu, X. Yang, C. Li, *Chem. Commun.* **2012**, *48*, 3686.
[121] H. P. Cong, J. F. Chen, S. H. Yu, *Chem. Soc. Rev.* **2014**, *43*, 7295.
[122] M. Nurunnabi, Z. Khatun, K. M. Huh, S. Y. Park, D. Y. Lee, K. J. Cho, Y. K. Lee, *ACS Nano* **2013**, *7*, 6858.
[123] C. Y. Wu, C. Wang, T. Han, X. J. Zhou, S. W. Guo, J. Y. Zhang, *Adv. Healthc. Mater.* **2013**, *2*, 1613.
[124] Z. Zeng, D. Yu, Z. He, J. Liu, F.-X. Xiao, Y. Zhang, R. Wang, D. Bhattacharyya, T. T. Y. Tan, *Sci. Rep.* **2016**, *6*. doi: 10.1038/srep20142.
[125] S. A. Kiran, Y. L. Thuyavan, G. Arthanareeswaran, T. Matsuurab, A. F. Ismail, *Chem. Eng. J.* **2016**, *286*, 528.
[126] L. Yu, Y. T. Zhang, B. Zhang, J. D. Liu, H. Q. Zhang, C. H. Song, *J. Membr. Sci.* **2013**, *447*, 452.
[127] Z. W. Xu, J. G. Zhang, M. J. Shan, Y. L. Li, B. D. Li, J. R. Niu, B. M. Zhou, X. M. Qian, *J. Membr. Sci.* **2014**, *458*, 1.